

Contents

1	Introduction	3
2	Literature Study	4
2.1	Stochastic MPC	4
2.2	Switching MPC	7
3	Background Theory	8
3.1	Probability Theory	8
3.1.1	Discrete Random Variables	9
3.1.2	Continuous Random Variables	12
3.2	Graph Theory	16
3.3	Probabilistic Graphical Models	17
3.3.1	Bayesian Networks	17
3.3.2	Dynamic Bayesian Networks	20
3.4	Control	22
3.4.1	Linear Quadratic Regulator Control	22
3.4.2	Reference Tracking	25
3.4.3	Linear Quadratic Gaussian Control	26
3.4.4	Model Predictive Control	27
3.5	Matrix Identities	28
4	Hidden Markov Models	29
4.1	Markov Models	29
4.2	Hidden Markov Models	30
4.2.1	Filtering	31
4.2.2	Smoothing	32
4.2.3	Viterbi Decoding	33
4.2.4	Prediction	34
4.3	Burglar Localisation Problem	36
5	CSTR Model	39
5.1	Qualitative Analysis	40
5.2	Nonlinear Model	41
5.3	Linearised Models	43
6	Inference using Linear Models	50
6.1	Filtering	51
6.2	Prediction	53
6.3	Smoothing and Viterbi Decoding	55
6.4	Filtering the CSTR	55
7	Inference using Nonlinear Models	60

7.1	Sequential Monte Carlo Methods	60
7.2	Particle Filter	64
7.3	Particle Prediction	66
7.4	Smoothing and Viterbi Decoding	66
7.5	Filtering the CSTR	66
8	Stochastic Linear Control	71
8.1	Unconstrained Stochastic Control	71
8.2	Constrained Stochastic Control	75
8.3	Reference Tracking	80
8.4	Linear System	80
8.5	Nonlinear System	87
8.6	Conclusion	95
9	Inference using Linear Hybrid Models	95
9.1	Exact Filtering	96
9.2	Rao-Blackwellised Particle Filter	96
9.3	Rao-Blackwellised Particle Prediction	98
9.4	Smoothing and Viterbi Decoding	98
9.5	Filtering the CSTR	99
10	Inference using Nonlinear Hybrid Models	109
10.1	Exact Inference	110
10.2	Approximate Inference	110
10.3	Particle Prediction	111
10.4	Filtering the CSTR	111
11	Stochastic Switching Linear Control	115
11.1	Current Literature	115
11.2	Unconstrained Control	115
11.3	Constrained Control	115
12	Conclusion	116

8 Stochastic Linear Control

In this section we consider the stochastic reference tracking problem. It is required to move the states and manipulated variables of the system, shown in (92), to the set point (x_{sp}, u_{sp}) by manipulating the input variables u .

$$\begin{aligned} x_{t+1} &= f(x_t, u_t) + w_{t+1} \\ y_{t+1} &= g(x_{t+1}) + v_{t+1} \end{aligned} \tag{92}$$

We assume uncorrelated zero mean additive Gaussian noise in both the state function f and the observation function g with known covariances W and V respectively. Clearly it is not possible to achieve perfect control (zero offset at steady state) because of the noise terms, specifically w_t . For this reason we need to relax the set point goal a little bit. We will be content if our controller is able to achieve Definition 8.1.

Definition 8.1. Stochastic Reference Tracking Goal: Suppose we have designed a controller and set $\delta > 0$ as a controller benchmark. If there exists some positive number $t^* < \infty$ such that $\forall t > t^*$ the controller input causes $\mathbb{E}[(x_t - x_{sp})^T Q(x_t - x_{sp}) + (u_t - u_{sp})^T R(u_t - u_{sp})] < \delta$ we will have satisfied the Stochastic Reference Tracking Goal given δ .

While Definition 8.1 is pleasing from a theoretical point of view, it is not easy to design a controller to specifically satisfy a given δ . We again simplify our goal somewhat: we will be content if the controller we design (without a specific δ in mind) can satisfy Definition 8.1 for some suitably small resultant δ . Intuitively, we would like the mean of the states and inputs to be “close enough” to the set points.

In this section we limit ourselves by only considering controllers developed using a single linear model of the underlying, possibly nonlinear, system functions f and g . The linearised model control is based upon is shown in (93) and is subject to the same noise as (92).

$$\begin{aligned} x_{t+1} &= Ax_t + Bu_t + w_{t+1} \\ y_{t+1} &= Cx_{t+1} + v_{t+1} \end{aligned} \tag{93}$$

We will endeavour to develop predictive controllers using the Graphical Models of Section 6 and 7.

8.1 Unconstrained Stochastic Control

Our first goal is to solve the problem in (94) given the current state estimate x_0 . If the system is controllable then solving (94) will satisfy the linear unconstrained Stochastic Reference Tracking Goal.

$$\begin{aligned} \min_{\mathbf{u}} J_{LQG}(x_0, \mathbf{u}) &= \mathbb{E} \left[\frac{1}{2} \sum_{k=0}^{N-1} (x_k^T Q x_k + u_k^T R u_k) + \frac{1}{2} x_N^T P_f x_N \right] \\ \text{subject to } x_{t+1} &= Ax_t + Bu_t + w_t \\ \text{and } y_t &= Cx_t + v_t \text{ (Observed)} \end{aligned} \tag{94}$$

Note that the future inputs $\mathbf{u} = (u_0, u_1, \dots, u_{T-1})$ are denoted in boldface to emphasise that it could be a vector of vectors. Inspecting (94) we see that this is none other than the LQG control problem of Section 3.4.3. Therefore we know what the optimal solution should look like.

We start our analysis using the results of Section 6. We immediately realise that the optimal linear state estimator is the Kalman Filter. We assume that at every sequential time step we have the current state estimate, supplied by the Kalman Filter, and denote this by x_0 . Since we are using the Kalman Filter the mean and covariance of the state estimate is well defined.

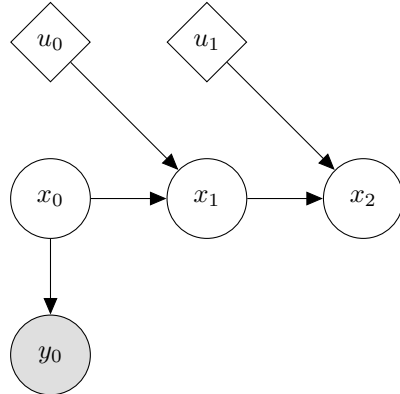


Figure 40: Graphical Model for state prediction

Inspecting Figure 40 we note that the state prediction equations derived in Subsection 6.2 are applicable. Thus we can predict the state distributions given the future inputs \mathbf{u} .

Before we proceed we prove a very intuitive result in Theorem 8.1. We will use this to link the predictive controller derived using the results of Section 6 to the LQR controller derived in Section 3.4.1. We provide two proofs, the second of which is more general than the first.

Theorem 8.1. Optimisation Equivalence Suppose we have two real valued convex objective functions $f(x_0, \mathbf{u})$ and $g(x_0, \mathbf{u})$ and we are required to minimise them with respect to \mathbf{u} over the same space where they are both defined: $\mathbf{u} \in \mathcal{U}$ and $x_0 \in \mathcal{X}$. Furthermore, suppose there exists a real number $k \geq 0$ such that $\forall \mathbf{u} \in \mathcal{U}$ we have that $g(x_0, \mathbf{u}) + k = f(x_0, \mathbf{u})$. Finally, assume the existence and uniqueness of the global minimiser for each problem. Then the global minimiser \mathbf{u}^* of $g(x_0, \mathbf{u})$ is also the global minimiser of $f(x_0, \mathbf{u})$.

Proof. This proof only holds over functions which are at least twice differentiable. By assumption we know that \mathbf{u}^* is the minimiser of $g(x_0, \mathbf{u})$ given x_0 . By the necessary conditions for optimality [20] we know that $\nabla g(x_0, \mathbf{u}^*) = 0$ and that $\nabla^2 g(x_0, \mathbf{u}^*)$ is positive semi-definite. Since f and g are both twice differentiable and $g(x_0, \mathbf{u}^*) + k = f(x_0, \mathbf{u}^*)$ it must hold that $\nabla g(x_0, \mathbf{u}^*) = \nabla f(x_0, \mathbf{u}^*)$ and $\nabla^2 g(x_0, \mathbf{u}^*) = \nabla^2 f(x_0, \mathbf{u}^*)$. Since $\nabla^2 g(x_0, \mathbf{u}^*)$ is positive semi-definite it must be that $\nabla^2 f(x_0, \mathbf{u}^*)$ is also positive semi-definite. Therefore \mathbf{u}^* is necessarily a minimum of f . Since f is convex the minimum must also be a global minimum. \square

Proof. This proof hold over differentiable and non-differentiable objective functions which are not necessarily convex. Suppose not i.e. there exists $\mathbf{u}_g \in \mathcal{U}$ such that $g(x_0, \mathbf{u}_g) < g(x_0, \mathbf{u}) \forall \mathbf{u} \in \mathcal{U}$ but $f(x_0, \mathbf{u}_g) \not< f(x_0, \mathbf{u}) \forall \mathbf{u} \in \mathcal{U}$. This implies that for $\mathbf{u}_f \in \mathcal{U}$ the global minimiser of f we have $f(x_0, \mathbf{u}_f) \leq f(x_0, \mathbf{u}_g)$.

Consider the case where $f(x_0, \mathbf{u}_f) = f(x_0, \mathbf{u}_g)$. This implies that both \mathbf{u}_f and \mathbf{u}_g are global minimisers of f and contradicts our assumption that the global minimiser is unique.

Consider the case where $f(x_0, \mathbf{u}_f) < f(x_0, \mathbf{u}_g)$. Since $g(x_0, \mathbf{u}) + k = f(x_0, \mathbf{u}) \forall \mathbf{u} \in \mathcal{U}$ this implies that $g(x_0, \mathbf{u}_f) < g(x_0, \mathbf{u}_g)$. But this contradicts our assumption that \mathbf{u}_g is the global minimiser of g .

It must then hold that $f(x_0, \mathbf{u}_g) < f(x_0, \mathbf{u}) \forall \mathbf{u} \in \mathcal{U}$. Therefore the global minimiser \mathbf{u}_g of $g(x_0, \mathbf{u})$ also minimises $f(x_0, \mathbf{u})$. Since f is convex the minimum must also be a global minimum. \square

Now we are in a position to show the equivalence between the LQR control problem and the LQG control problem using the results of Section 6. Theorem 8.2 shows how this is possible. It is quite reassuring to note that by starting within the framework of Graphical Models we arrive at the most important contribution of [47] and [48] in an intuitively simple manner.

Theorem 8.2. LQR and LQG Objective Function Difference Consider the LQR and LQG Objective Functions in (95) and (96) respectively.

$$J_{LQR}(x_0, \mathbf{u}) = \frac{1}{2} \sum_{k=0}^{N-1} (x_k^T Q x_k + u_k^T R u_k) + \frac{1}{2} x_N^T P_f x_N \quad (95)$$

with $x_{t+1} = Ax_t + Bu_t$ (Observed)

$$J_{LQG}(x_0, \mathbf{u}) = \mathbb{E} \left[\frac{1}{2} \sum_{k=0}^{N-1} (x_k^T Q x_k + u_k^T R u_k) + \frac{1}{2} x_N^T P_f x_N \right] \quad (96)$$

with $x_{t+1} = Ax_t + Bu_t + w_{t+1}$

and $y_t = Cx_t + v_t$ (Observed)

Suppose x_0 is the state estimate supplied by the Kalman Filter given the latest observation in the stochastic case. In the deterministic case we have that $x_0 = \mathbb{E}[x_0] = \mu_0$ because we exactly observe the state. Given any input sequence $\mathbf{u} \in \mathcal{U}$, where \mathcal{U} is the shared admissible input space, we have that $J_{LQR}(x_0, \mathbf{u}) + \frac{1}{2} \sum_{k=0}^N \text{tr}(Q\Sigma_k) = J_{LQG}(x_0, \mathbf{u})$ where $\Sigma_{t+1} = W + A\Sigma_t A^T$ and Σ_0 is the covariance matrix of the current state given by the Kalman Filter.

Proof. Expanding the LQG objective function and noting that \mathbf{u} is deterministic we have (97). Note that the conditional expectations in the expansion originate from the graphical

model in Figure 40 due to the first order Markov assumption.

$$\begin{aligned}
J_{LQG}(x_0, \mathbf{u}) &= \frac{1}{2} \mathbb{E} [x_0^T Q x_0 + u_0^T R u_0] + \frac{1}{2} \mathbb{E} [x_1^T Q x_1 + u_1^T R u_1 | x_0] + \dots \\
&\quad + \frac{1}{2} \mathbb{E} [x_{N-1}^T Q x_{N-1} + u_{N-1}^T R u_{N-1} | x_{N-2}] + \frac{1}{2} \mathbb{E} [x_N^T P_f x_N | x_{N-1}] \\
&= \frac{1}{2} \mathbb{E} [x_0^T Q x_0] + \frac{1}{2} u_0^T R u_0 + \frac{1}{2} \mathbb{E} [x_1^T Q x_1 | x_0] + \frac{1}{2} u_1^T R u_1 + \dots \\
&\quad + \frac{1}{2} \mathbb{E} [x_{N-1}^T Q x_{N-1} | x_{N-2}] + \frac{1}{2} u_{N-1}^T R u_{N-1} + \frac{1}{2} \mathbb{E} [x_N^T P_f x_N | x_{N-1}]
\end{aligned} \tag{97}$$

We know that $x_0 \sim \mathcal{N}(\mu_0, \Sigma_0)$ because the current state estimate comes from the Kalman Filter. This means that we can evaluate the first expected value in (97) using Theorem 3.5 as shown in (98).

$$\mathbb{E} [x_0^T Q x_0] = \text{tr}(Q \Sigma_0) + \mu_0^T Q \mu_0 \tag{98}$$

Now we turn our attention to the second expected value in (97). First note that because we have x_0 and \mathbf{u} we can use the result from Section 6.2 to predict (optimally) the distribution of x_1 . Therefore we know that $x_1 \sim \mathcal{N}(A\mu_0 + Bu_0, W + A\Sigma_0 A^T)$. Now we let $\mu_1 = A\mu_0 + Bu_0$ and $\Sigma_0 = W + A\Sigma_0 A^T$. Then by using Theorem 3.5 as before we have (99).

$$\mathbb{E} [x_1^T Q x_1 | x_0] = \text{tr}(Q \Sigma_1) + \mu_1^T Q \mu_1 \tag{99}$$

Note that $\text{tr}(Q \Sigma_1)$ does not depend on u_0 but only on the initial state estimate x_0 which is independent of the future inputs \mathbf{u} . Notice that we can continue in this manner to simplify the LQG objective function to (100).

$$\begin{aligned}
J_{LQG}(x_0, \mathbf{u}) &= \frac{1}{2} \sum_{k=0}^{N-1} (\mu_k^T Q \mu_k + u_k^T R u_k) + \frac{1}{2} \mu_N^T P_f \mu_N + \frac{1}{2} \sum_{k=0}^N \text{tr}(Q \Sigma_k)
\end{aligned} \tag{100}$$

with $\mu_{t+1} = A\mu_t + Bu_t$

and $\Sigma_{t+1} = W + A\Sigma_t A^T$

Now note that except for the last term $J_{LQG}(x_0, \mathbf{u})$ is exactly the same as $J_{LQR}(x_0, \mathbf{u})$. The conclusion follows because $\frac{1}{2} \sum_{k=0}^N \text{tr}(Q \Sigma_k)$ is independent of \mathbf{u} . \square

Finally we combine Theorem 8.1 and 8.2 to produce Theorem 8.3 which is the main result of this subsection.

Theorem 8.3. Solution of the Finite Horizon LQG control problem We wish to solve the LQG control problem within the framework of Graphical Models. The full problem is shown in (101).

$$\begin{aligned}
\min_{\mathbf{u}} V(x_0, \mathbf{u}) &= \mathbb{E} \left[\frac{1}{2} \sum_{k=0}^{N-1} (x_k^T Q x_k + u_k^T R u_k) + \frac{1}{2} x_N^T P_f x_N \right] \\
\text{subject to } x_{t+1} &= Ax_t + Bu_t + w_t \\
\text{and } y_t &= Cx_t + v_t \text{ (Observed)}
\end{aligned} \tag{101}$$

The solution of (101) is equivalent to solving the LQR problem with initial state equal to the mean of the initial state estimate from the Kalman Filter.

Proof. We assume that we have the Kalman Filter state estimate for x_0 . We use Theorem 8.2 to prove that given x_0 and $\forall \mathbf{u} \in \mathcal{U}$ we have that $J_{LQR}(x_0, \mathbf{u}) + \frac{1}{2} \sum_{k=0}^N \text{tr}(Q\Sigma_k) = J_{LQG}(x_0, \mathbf{u})$ with $\frac{1}{2} \sum_{k=0}^N \text{tr}(Q\Sigma_k) \in \mathbb{R}$ a constant depending only on x_0 . Thus we can use Theorem 8.1 to prove that we only need to solve for the optimal controller input \mathbf{u}^0 using the LQR objective function. Thus we can use Theorem 3.11 to find \mathbf{u} . \square

As we have mentioned before, the Separation Theorem implies that the solution of the LQG control problem is achieved by using the Kalman Filter to optimally estimate the current state and then using that state estimate in the optimal LQR controller. It is reassuring that Theorem 8.3 is confirmed by this result. The primary benefit of the Graphical Model approach is clear: we have solved the LQG problem without resorting to Stochastic Dynamical Programming.

Under some circumstances it is also possible to extend the result of Theorem 8.3 to the infinite horizon case as shown in Theorem 8.4.

Theorem 8.4. Solution of the Infinite Horizon LQG control problem If the linear model of (93) is stable then, using, with some minor adjustments, Theorems 8.1 and 8.2 it is possible to show that the infinite horizon LQG problem is solved in a similar manner: the Kalman Filter state estimate is used in conjunction with the infinite horizon LQR solution. This result can also be obtained by using the Separation Theorem.

To clarify why it is important that the linear system, i.e. the matrix A , is stable, consider the quantity $\frac{1}{2} \sum_{k=0}^N \text{tr}(Q\Sigma_k)$. If it is unbounded the optimisation minimum will tend to infinity. Inspecting $\Sigma_{t+1} = W + A\Sigma_t A^T$ we see that $\|\Sigma_\infty\|$ will be unbounded if $\|A\Sigma_t A^T\|$ becomes unbounded (W is a constant). Note that $\|\cdot\|$ is some matrix norm. It can be shown that if the eigenvalues of A are less than unity i.e. the linear model is stable, then $\|A\Sigma_{t+1} A^T\| \leq \|A\Sigma_t A^T\|$ which implies that $\frac{1}{2} \sum_{k=0}^N \text{tr}(Q\Sigma_k)$ is bounded and the optimisation is reasonable.

8.2 Constrained Stochastic Control

The goal of this section is to solve the stochastic constrained optimisation problem shown in (102). We assume that the underlying system is linear and the probability distributions are Gaussian⁷. We also restrict our analysis to affine constraints. Note that we only include one constraint in the succeeding analysis however, additional constraints are handled in exactly

⁷From the results of Section 6 the probability distributions will be Gaussian if the system dynamics are linear. However, it is well known [32] that MPC is not in general a linear controller. From an analytical point of view this is problematic. We assume that the nonlinearity introduced by the MPC is negligible.

the same way as we will show.

$$\begin{aligned}
& \min_{\mathbf{u}} \mathbb{E} \left[\frac{1}{2} \sum_{k=0}^{N-1} (x_k^T Q x_k + u_k^T R u_k) + \frac{1}{2} x_N^T P_f x_N \right] \\
& \text{subject to } x_{t+1} = Ax_t + Bu_t + w_t \\
& \text{and } y_t = Cx_t + v_t \text{ (Observed)} \\
& \text{and } \mathbb{E}[d^T x_t + e] \geq 0 \forall t = 1, \dots, N \\
& \text{and } \Pr(d^T x_t + e \geq 0) \geq p \forall t = 1, \dots, N
\end{aligned} \tag{102}$$

It might seem that the last constraint is a duplicate of the preceding one. Closer inspection reveals their different character. The first inequality constraint requires that the predicted states satisfy the constraint “on average” while the second inequality constraint requires that the predicted states jointly satisfy the constraint with at least some probability p .

Theorem 8.5 succinctly shows that it is simple to convert the first stochastic constraint in (102) to a linear deterministic constraint.

Theorem 8.5. Affine Expected Value Constraints Suppose we have a stochastic variable x with a known Gaussian distribution. Then the stochastic constraint $\mathbb{E}[d^T x + e] \geq 0$ simplifies to the deterministic constraint $d^T \mu + e \geq 0$ where $\mathbb{E}[x] = \mu$ is the mean of the stochastic variable.

Proof. We know that x is a Gaussian stochastic variable. By the results of Section 3.5 we know that $\mathbb{E}[d^T x + e] = d^T \mu + e$. This immediately implies the Theorem. \square

It is interesting to pause here for a moment and consider Theorem 8.3 and Theorem 8.5 applied to a problem of the form (103). We assume that the current state estimate is available at each time step and that $\mathbb{E}[x_0] = \mu_0$.

$$\begin{aligned}
& \min_{\mathbf{u}} \mathbb{E} \left[\frac{1}{2} \sum_{k=0}^{N-1} (x_k^T Q x_k + u_k^T R u_k) + \frac{1}{2} x_N^T P_f x_N \right] \\
& \text{subject to } x_{t+1} = Ax_t + Bu_t + w_t \\
& \text{and } y_t = Cx_t + v_t \text{ (Observed)} \\
& \text{and } \mathbb{E}[d^T x_t + e] \geq 0 \forall t = 1, \dots, N
\end{aligned} \tag{103}$$

It is clear that by applying those two theorems it is possible to rewrite (103) as (104).

$$\begin{aligned}
& \min_{\mathbf{u}} \frac{1}{2} \sum_{k=0}^{N-1} (\mu_k^T Q \mu_k + u_k^T R u_k) + \frac{1}{2} \mu_N^T P_f \mu_N + \frac{1}{2} \sum_{k=0}^N \text{tr}(Q \Sigma_k) \\
& \text{subject to } \mu_{t+1} = A\mu_t + Bu_t \\
& \text{and } d^T \mu_t + e \geq 0 \forall t = 1, \dots, N
\end{aligned} \tag{104}$$

This implies that the standard deterministic MPC problem (104) is equivalent to the stochastic MPC problem with affine expected value constraints (103) under the assumptions of linearity and normality. This suggests that if probability constraints are not required that standard deterministic MPC will be sufficient for control.

Theorem 8.6 is a necessary step before we can convert the last stochastic inequality constraint of (102) into a nonlinear deterministic constraint.

Theorem 8.6. Shortest Squared Mahalanobis Distance between a Hyperplane and a Point Suppose we are given a symmetric positive semi-definite matrix S and a point y . The shortest squared Mahalanobis Distance between y and the hyperplane $b^T x + c = 0$ is given by $\frac{(b^T y + c)^2}{b^T S b}$.

Proof. It is natural to formulate Theorem 8.6 as an optimisation problem as shown in (105).

$$\begin{aligned} \min_x \quad & (x - y)^T S^{-1} (x - y) \\ \text{subject to } & b^T x + c = 0 \end{aligned} \tag{105}$$

Note that S and therefore also S^{-1} is symmetric. Using conventional calculus we have $\nabla f(x) = (S^{-1} + S^{-1}{}^T)x - 2S^{-1}y = 2S^{-1}x - 2S^{-1}y$ and $\nabla g(x) = b^T$. Using the method of Lagrangian Multipliers [20] we have the system of equations (106)

$$\begin{aligned} 2S^{-1}x - 2S^{-1}y + \lambda b = 0 \\ b^T x + c = 0 \end{aligned} \tag{106}$$

This can be rewritten in block matrix form as shown in (107).

$$\begin{pmatrix} 2S^{-1} & b \\ b^T & 0 \end{pmatrix} \begin{pmatrix} x \\ \lambda \end{pmatrix} = \begin{pmatrix} 2S^{-1}y \\ -c \end{pmatrix} \tag{107}$$

The special structure of the left hand side matrix in (107) allows us to analytically compute the inverse (see Theorem 3.13 in Section 3.5) as shown in (108).

$$\begin{pmatrix} 2S^{-1} & b \\ b^T & 0 \end{pmatrix}^{-1} = \begin{pmatrix} \frac{1}{2}S(I - \frac{bb^T S}{b^T S b}) & \frac{Sb}{b^T S b} \\ \frac{b^T S}{b^T S b} & -\frac{2}{b^T S b} \end{pmatrix} \tag{108}$$

To find the arguments which satisfy (106) we solve (109) which is equivalent to solving the system of linear equations in (107).

$$\begin{pmatrix} \frac{1}{2}S(I - \frac{bb^T S}{b^T S b}) & \frac{Sb}{b^T S b} \\ \frac{b^T S}{b^T S b} & -\frac{2}{b^T S b} \end{pmatrix} \begin{pmatrix} 2S^{-1}y \\ -c \end{pmatrix} = \begin{pmatrix} S(I - \frac{bb^T S}{b^T S b})S^{-1}y - c \frac{Sb}{b^T S b} \\ 2(\frac{b^T S}{b^T S b} + \frac{c}{b^T S b}) \end{pmatrix} \tag{109}$$

Therefore, the arguments which minimise (105) are $x^* = S(I - \frac{bb^T S}{b^T S b})S^{-1}y - c \frac{Sb}{b^T S b}$. Substi-

tuting this into the objective function we have (110).

$$\begin{aligned}
& (x^* - y)^T S^{-1} (x^* - y) \\
&= \left(S \left(I - \frac{bb^T S}{b^T S b} \right) S^{-1} y - c \frac{Sb}{b^T S b} - y \right)^T S^{-1} \left(S \left(I - \frac{bb^T S}{b^T S b} \right) S^{-1} y - c \frac{Sb}{b^T S b} - y \right) \\
&= \left(\frac{Sbb^T y}{b^T S b} + c \frac{Sb}{b^T S b} \right)^T S^{-1} \left(\frac{Sbb^T y}{b^T S b} + c \frac{Sb}{b^T S b} \right) \\
&= \frac{(Sb)^T}{b^T S b} (b^T y + c)^T S^{-1} \frac{Sb}{b^T S b} (b^T y + c) \\
&= \frac{b^T S}{b^T S b} (b^T y + c)^T \frac{b}{b^T S b} (b^T y + c) \\
&= (b^T y + c)^T \frac{b^T S b}{(b^T S b)^2} (b^T y + c) \\
&= \frac{(b^T y + c)^T (b^T y + c)}{b^T S b} \\
&= \frac{(b^T y + c)^2}{b^T S b}
\end{aligned} \tag{110}$$

We can conclude that the shortest squared Mahalanobis Distance between a point y and the constraint of (105) is $\frac{(b^T y + c)^2}{b^T S b}$. \square

In Theorem 8.7 we apply Theorem 8.6 to convert the stochastic constraints into nonlinear deterministic constraints.

Theorem 8.7. Gaussian Affine Chance Constraints If the underlying distribution of a random variable x is Gaussian then the chance constraint $\Pr(d^T x + e \geq 0) \geq p$ can be rewritten as the deterministic constraint $\frac{(d^T \mu + e)^2}{d^T S d} \geq k^2$ where k^2 is the (constant) critical value of the inverse cumulative Chi-Squared Distribution with the degrees of freedom equal to the dimensionality of x such that $\Pr(\mathcal{X} \leq k^2) = p$.

Proof. Intuitively Theorem 8.7 posits that if the shortest squared Mahalanobis distance is further away than some threshold k^2 the chance constraint $\Pr(dx + e \geq 0) \geq p$ will be satisfied. Since x is a Gaussian stochastic variable we have that $\mathbb{E}[x] = \mu$ and $\text{var}[x] = \Sigma$. Let $\Omega = \{x \in \mathbb{R}^n \mid (x - \mu)^T \Sigma^{-1} (x - \mu) \leq k^2\}$ and k^2 be the critical value such that for the Chi-Squared Distribution with degrees of freedom equal to the dimension of x we have that $\Pr(\mathcal{X} \leq k^2) = p$. Then it is well known [40] that $\int_{\Omega} p(x|\mu, \Sigma) dx = p$ where $p(\cdot|\mu, \Sigma)$ is the multivariate Gaussian probability distribution function of x . If the shortest squared Mahalanobis Distance from the mean of x is further away from the affine constraint $d^T z + e = 0$ than k^2 it implies that the curve of the function $h(z) = (z - \mu)^T \Sigma^{-1} (z - \mu) = k^2$ does not intersect with the constraint. This implies, with at least a probability of p , that the chance constraint will not be violated because the “confidence ellipse” does not intersect the constraint. See Figure for a diagram of the principle behind Theorem 8.7 [13]. **insert picture** \square

It is interesting to note the striking similarity between the work in [45] and [44] and Theorem 8.7 given that we started analysing the problem within the framework of Graphical Models.

The additional benefit of Theorem 8.7 is that it formulates the stochastic constraint as a function of the statistical Mahalanobis Distance measure. This is useful because it lends a statistical interpretation to Theorem 8.7 even if the underlying distribution is non-Gaussian.

In Theorem 8.8 we combine and elaborate on the work of [47], [45] to yield a QP MPC which exactly satisfies the stochastic MPC in (102) given the assumptions of linearity and normality. Note that the dimensionality of the problem is arbitrary.

Theorem 8.8. Conversion of the Stochastic MPC formulation to the standard deterministic QP MPC formulation Under the assumptions of linearity and Gaussian distributions we can reformulate the stochastic MPC problem shown in (102) as a standard deterministic QP MPC problem shown in (111).

$$\begin{aligned} \min_{\mathbf{u}} \frac{1}{2} \sum_{k=0}^{N-1} (\mu_k^T Q \mu_k + u_k^T R u_k) + \frac{1}{2} \mu_N^T P_f \mu_N + \frac{1}{2} \sum_{k=0}^N \text{tr}(Q \Sigma_k) \\ \text{subject to } \mu_{t+1} = A \mu_t + B u_t \\ \text{and } \Sigma_{t+1} = W + A \Sigma_t A^T \\ \text{and } d^T \mu_t + e \geq k \sqrt{d^T \Sigma_t d} \quad \forall t = 1, \dots, N \end{aligned} \tag{111}$$

Other deterministic constraints, e.g. on the input, can be added as usual. Note that we have assumed that the initial state estimate x_0 is available in the form of its mean, μ_0 , and covariance, Σ_0 . It is straightforward to include more chance constraints. Since each chance constraint is reduced to an inequality constraint which measures the Mahalanobis Distance between the predicted distributions, the resultant feasible points will jointly satisfy all chance constraints.

Proof. Let the admissible set of controller inputs \mathcal{U} be the same for both the stochastic MPC and the deterministic MPC formulations. Furthermore, let the current state estimate x_0 be given. Then by Theorem 8.2 the objective function and equality constraints follow. By Theorem 8.5 the first inequality constraint in (102) can be reformulated to require that $d^T \mu + e \geq 0$. The last inequality constraint in (102) follows from Theorem 8.7 as shown in (112).

$$\begin{aligned} \frac{(d^T \mu + e)^2}{d^T S d} \geq k^2 &\implies (d^T \mu + e)^2 \geq k^2 d^T S d \\ &\implies d^T \mu + e \geq k \sqrt{d^T S d} \end{aligned} \tag{112}$$

The first line of (112) follows because S is positive semi-definite and $d \neq 0$ (otherwise it would not be a constraint), therefore it can be multiplied over the inequality sign like a positive number. The second line follows because of the first inequality constraint: we know that $d^T \mu + e \geq 0$ and therefore we can square root both sides of the inequality constraint. Thus we have the two inequality constraints $d^T \mu + e \geq 0$ and $d^T \mu + e \geq k \sqrt{d^T S d}$. Since $k > 0$ (otherwise we do not have a meaningful chance constraint) we can condense the two inequality constraints into a single constraint: $d^T \mu + e \geq k \sqrt{d^T S d} > 0$ from which the conclusion follows. \square

The beauty of Theorem 8.8 is that no new theory is necessary to analyse the stability and convergence results of the new MPC. This is highly desirable because it allows one to merely “add” the last inequality constraint to your existing MPC formulation. Most practical MPCs will have some form of state estimation and thus no new parameters are introduced either. Since the problem is in standard QP form it is straightforward to implement and, even more importantly, it is computationally fast because the problem is trivially convex.

In the work by [47] and [48] it is found that feasibility problems might arise if one uses the predicted covariance estimates in the controller. If the system is unstable the uncertainty in the estimates can grow with time as discussed in Theorem 8.4. This can cause the ellipses used in Theorem 8.7 to become too large to fit inside the feasible region. The approach adopted by [47] and [48] is to only use the one step ahead predicted covariance (Σ_1) over the entire prediction horizon. This does not ensure feasibility but restricts the growth associated with infeasibility. The drawback of this approach is that it might cause constraint violation because the controller will be more aggressive.

8.3 Reference Tracking

So far we have only dealt with controllers which would drive the system to the origin. The more general situation we are interested in is arbitrary reference point tracking. Fortunately, Section 3.4.2 applies without modification because we managed to cast the Stochastic MPC problem into a deterministic MPC problem.

8.4 Linear System

In this section we consider the problem of controlling a linear system using the stochastic MPC formulation of Theorem 8.8. More precisely, we assume the linear model linearised about the unsteady operating point of our CSTR example from Section 5 accurately represents the underlying system. For the purposes of illustration we will only use the (somewhat unrealistic) system where both states are measured. However, there is no theoretical reason why we cannot use the system where only temperature is measured. The drawback of using the latter system is that inference, as discussed previously, will be worse. The control goal is to steer the concentration, in the sense of Definition 8.1, to the unsteady operating point ($C_A = 0.49 \text{ kmol.m}^{-3}$) about which the system was linearised. See Section 5 for more details.

We repeat the relevant system dynamics in (113) using a time step $h = 0.1$.

$$\begin{aligned} A &= \begin{pmatrix} 0.9959 & -6.0308 \times 10^{-5} \\ 0.4186 & 1.0100 \end{pmatrix} & B &= \begin{pmatrix} 0 \\ 8.4102 \times 10^{-5} \end{pmatrix} & C &= \begin{pmatrix} 1 & 0 \\ 0 & 1 \end{pmatrix} \\ W &= \begin{pmatrix} 1 \times 10^{-6} & 0 \\ 0 & 0.1 \end{pmatrix} & V &= \begin{pmatrix} 1 \times 10^{-3} & 0 \\ 0 & 10 \end{pmatrix} \end{aligned} \tag{113}$$

The tuning parameters used in this and all subsequent sections are shown in (114). Note that the magnitude difference between the components of Q , P_f and R is necessary because the units of concentration and heat input are not scaled.

$$Q = P_f = \begin{pmatrix} 1 \times 10^4 & 0 \\ 0 & 0 \end{pmatrix} \quad R = \left(1 \times 10^{-6} \right) \quad (114)$$

We assume that a Kalman Filter supplies the initial state estimate x_0 and that the mean μ_0 of that estimate is used for control. Additionally, we assume a zero order hold of 1 min between controller inputs.

Firstly we illustrate the approach of using only the result of Theorem 8.3 i.e. we apply the LQG regulator to the system. Based on our previous results we know that given the Kalman Filter state estimate mean μ_0 we only need to solve the LQR as shown in (115) to solve the LQG problem.

$$\min_{\mathbf{u}} \frac{1}{2} \sum_{k=0}^{N-1} (\mu_k^T Q \mu_k + u_k^T R u_k) + \frac{1}{2} \mu_N^T P_f \mu_N \quad (115)$$

subject to $\mu_{t+1} = A\mu_t + Bu_t$

Figure 41 shows that the system does indeed converge, noisily, to the set point. The primary drawback of this method is that there is no easy way to constrain the system. From a practical perspective this can be problematic.

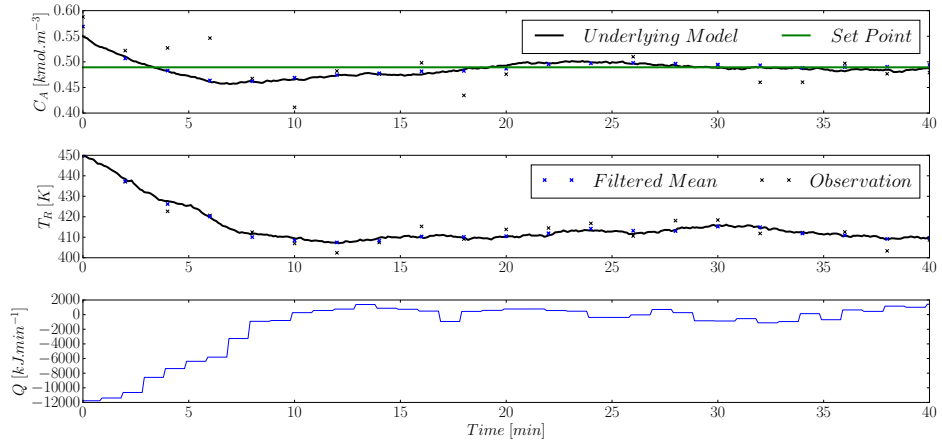


Figure 41: Unconstrained LQG regulator tracking with initial condition $(0.55, 450)$ and measuring both states.

The average heat energy usage (controller input) over the simulation run is 214 kJ/min. The average set point error is 2.38% over the same 40 min time period⁸.

Next we illustrate the approach of using conventional deterministic MPC to control the stochastic system. The MPC formulation is shown in (116). Using MPC allows us to easily

⁸We define the average energy input by $\frac{h}{N} \sum_{t=0}^N |u_t - u_s|$ and the average concentration error by $\frac{1}{N} \sum_{t=0}^N \left| \frac{C_{At} - y_{sp}}{y_{sp}} \right|$

add state and input constraints; this is a significant improvement over conventional LQG as discussed previously.

$$\begin{aligned}
& \min_{\mathbf{u}} \frac{1}{2} \sum_{k=0}^{N-1} (\mu_k^T Q \mu_k + u_k^T R u_k) + \frac{1}{2} \mu_N^T P_f \mu_N \\
& \text{subject to } \mu_{t+1} = A\mu_t + B u_t \\
& \text{and } \begin{pmatrix} 10 \\ 1 \end{pmatrix}^T \mu_t + 411 \geq 0 \quad \forall t = 1, \dots, N \\
& \text{and } |u_t| \leq 10000 \quad \forall t = 0, \dots, N-1
\end{aligned} \tag{116}$$

We only use a single state constraint in this dissertation but the extension to multiple constraints is straightforward. The prediction and control horizon are equal to each other and set at 150 time steps i.e. 15 minutes into the future. We additionally constrain the magnitude of the inputs.

Since we have assumed normality the deterministic state inequality constraint can also be seen as an affine expected value constraint as shown in Theorem 8.5.

In Figure 42 we see the reference tracking and controller input for the deterministic MPC. The average heat energy input and set point error over the simulation run is 2.70% and 222 kJ/min. Interestingly the average error is not much different but the controller requires more energy to track the setpoint without violating the constraints. This is reasonable because the additional constraints make problem (116) a harder problem than (115).

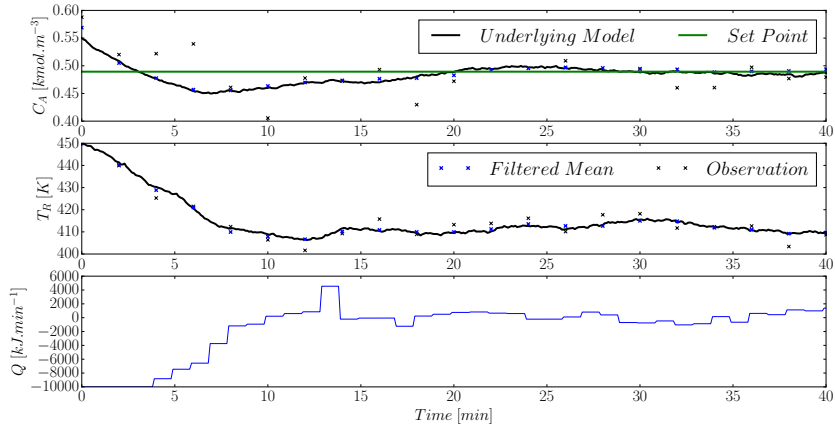


Figure 42: Deterministic constrained MPC tracking with initial condition (0.55, 450) and measuring both states.

Like the LQG controller, it is clear that we have noisy convergence to the set point. As mentioned previously we will never be able to achieve zero set point offset because of the noise term in the system dynamics (92). Note that we have constrained the maximum magnitude of the inputs such that $|u_t| \leq 10000$ kJ/min. In the unconstrained case the controller required a maximum absolute input magnitude of over 12000 kJ/min; the ability to naturally constrain the input can be practically very useful. The benefit of MPC is apparent here.

In Figure 43 we see the corresponding state space trajectory of the system together with the state constraint.

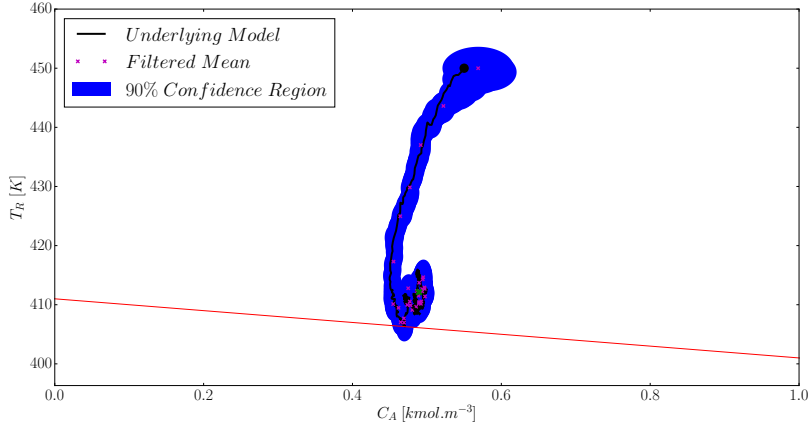


Figure 43: Deterministic MPC state space trajectory with initial condition $(0.55, 450)$ and measuring both states.

While the predicted mean state estimates do not violate the constraint (due to the optimisation constraints) the actual underlying system does. This is clearly seen if one inspects the confidence region around the lower state estimates. The confidence region is deeply violated by the constraint which implies that it is likely that the underlying system might. This is clearly a problem from a control point of view; the deterministic MPC cannot ensure that the constraint is satisfied.

We remedy this situation by introducing the stochastic MPC as discussed in Theorem 8.8 and shown in (117) for convenience. Note that $d^T = (10, 1)$ and $e = 411$ as before. By consulting a Chi-Squared Distribution table we set $k^2 = 4.6052$ which corresponds to the chance constraint $\Pr(d^T x_t + e \geq 0) \geq 90\% \forall t = 1, \dots, N$.

$$\begin{aligned} \min_{\mathbf{u}} \quad & \frac{1}{2} \sum_{k=0}^{N-1} (\mu_k^T Q \mu_k + u_k^T R u_k) + \frac{1}{2} \mu_N^T P_f \mu_N + \frac{1}{2} \sum_{k=0}^N \text{tr}(Q \Sigma_k) \\ \text{subject to } & \mu_{t+1} = A \mu_t + B u_t \\ \text{and } & \Sigma_{t+1} = W + A \Sigma_t A^T \\ \text{and } & d^T \mu_t + e \geq k \sqrt{d^T \Sigma_t d} \quad \forall t = 1, \dots, N \\ \text{and } & |u_t| \leq 10000 \quad \forall t = 0, \dots, N-1 \end{aligned} \tag{117}$$

Note that problem (117) is harder than (116) due to the added constraint and thus we expect that the system will require greater controller input to satisfy the constraint.

In Figure 44 we see that the stochastic MPC is able to track the set point in a similar manner as the LQG controller and deterministic MPC. The total average heat input and set point error over the simulation run is 290 kJ/min and 2.95% respectively. This problem is harder than the preceding one due to the additional constraint and thus more energy is required.

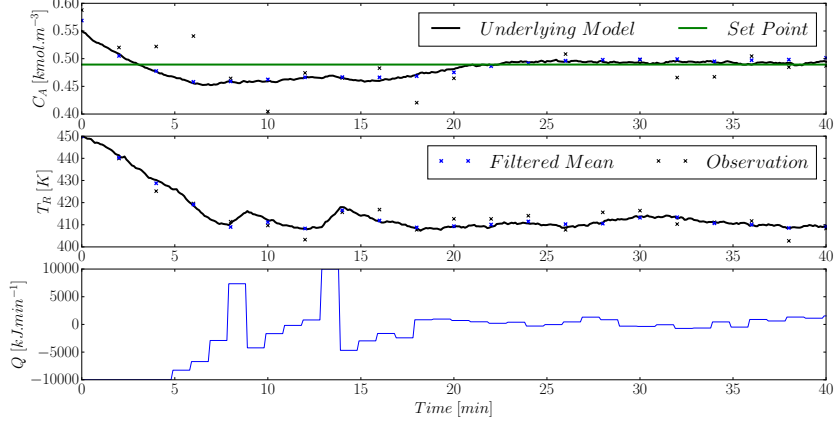


Figure 44: Stochastic constrained MPC tracking with initial condition $(0.55, 450)$ and measuring both states. A Kalman Filter is used for inference and the chance constraint is set at 90%.

However, the benefit of adding the stochastic constraint is apparent in Figure 45. It is clear that the constraint on the underlying state is not violated.

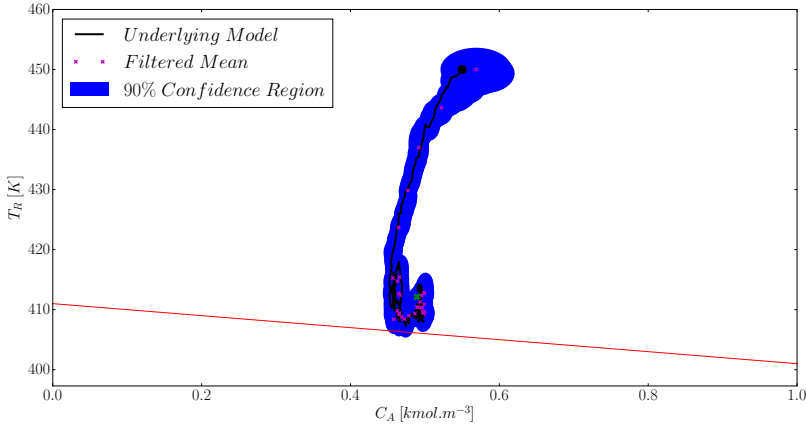


Figure 45: Stochastic constrained MPC state space trajectory with initial condition $(0.55, 450)$ and measuring both states. A Kalman Filter is used for inference and the chance constraint is set at 90%.

Since the stochastic constraint is only enforced with probability 90% it is possible that the underlying system can come “close” to the constraint. This then has the consequence that the posterior confidence region marginally violates (spills over) the constraint as seen in the lower regions of Figure 45.

It is interesting to investigate what effect increasing the probability that the chance constraint is satisfied will have on the system. To this end we modify the chance constraint of (117) such that $k^2 = 13.8155$ which corresponds to the chance constraint $\Pr(d^T x_t + e \geq 0) \geq 99.9\% \forall t = 1, \dots, N$. We expect that the underlying system will be moved further away from

constraint due to this added level of conservativeness.

In Figure 46 we see that the stochastic MPC still tracks the set point and Figure 47 shows that the expected behaviour is realised.

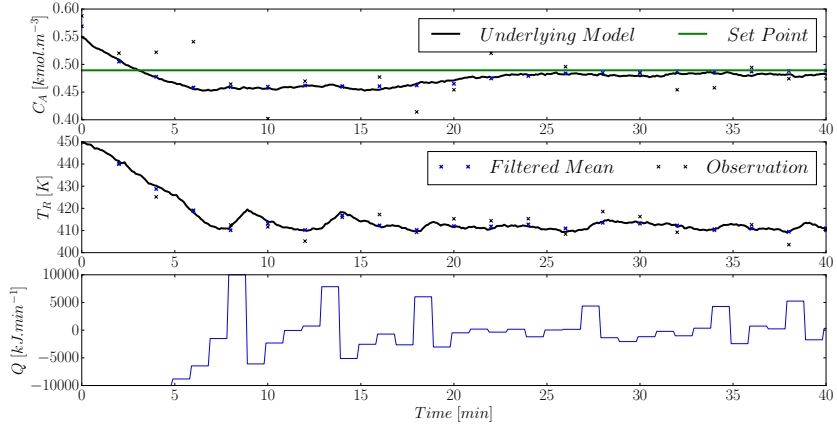


Figure 46: Stochastic constrained MPC tracking with initial condition $(0.55, 450)$ and measuring both states. A Kalman Filter is used for inference and the chance constraint is set at 99.9%.

The average heat input and average set point error is 3.73% and 351 kJ/min. The added conservativeness of the MPC prevents it from attempting to get to the set point as fast as the previous stochastic MPC; this causes the higher average error but the constraints are satisfied more robustly. As before, the control problem is harder and thus requires more energy.

In Figure 47 we see the 90% confidence region is above the constraint. Since the probability that the predicted states are close to the constraint is much lower than before we see that the confidence region satisfies the constraint everywhere.

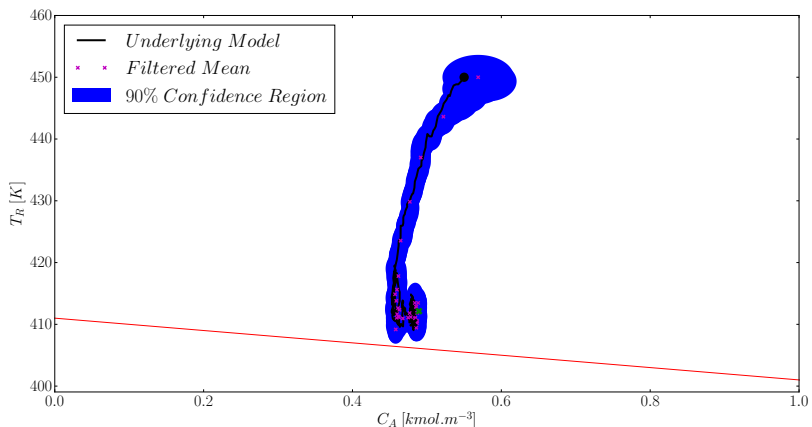


Figure 47: Stochastic constrained MPC state space trajectory with initial condition $(0.55, 450)$ and measuring both states. A Kalman Filter is used for inference and the chance constraint is set at 99.9%.

It would also be correct to infer that k can be used as an empirical measure of the inherent stochastic conservativeness of the resulting controller. That is, lower values of k indicate a more aggressive controller which may violate the chance constraints and higher values of k indicate a more conservative controller. This can be useful for systems where the normal assumption is not valid but one would still like to enforce stochastic constraints in some empirical sense.

We have made the strong assumption that the system dynamics remain linear and Gaussian even under the MPC control law which is not necessarily linear [32]. Clearly if the system is far from Gaussian the Gaussian approach to simplifying the chance constraint will not be valid. Fortunately this is relatively simple to check and serves as a good way of measuring controller health. That is, the more Gaussian the filtered distributions are, the better the linear stochastic controller will work.

Kullback-Leibler Divergence was introduced in Theorem 3.8 to estimate the degree to which samples match a given distribution. From Section 7 we know that given enough particles a Particle Filter can accurately represent any distribution. Thus we temporarily replace the Kalman Filter with a Particle filter and use Theorem 3.8 to estimate the degree of normality of the posterior state distributions.

Figure 48 shows the degree to which the underlying distribution is Gaussian. Since we cannot use an infinite amount of particles we compare the sampled Gaussian distribution approximation to a baseline.

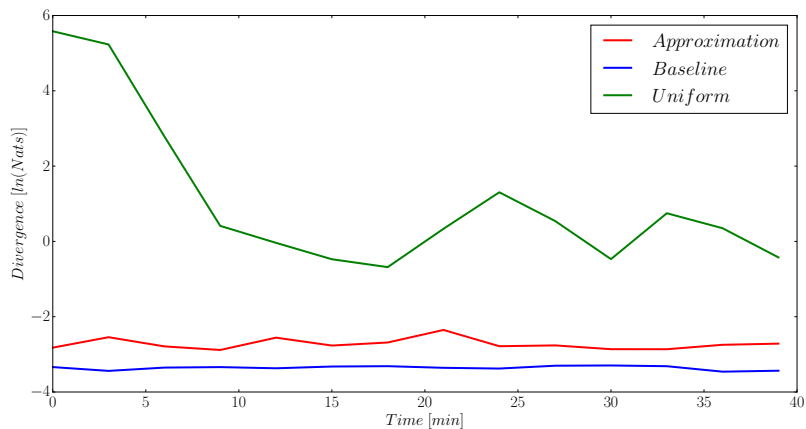


Figure 48: Kullback-Leibler Divergence between the assumed Gaussian distribution and different sampled distributions using 5000 particles. The underlying model is linear. A log scale is used because the uniform curve differs by more than an order of magnitude from the other curves.

The approximation curve in Figure 48 shows how much the samples diverge from the Gaussian distribution approximated using the samples. The baseline curve shows how much the Gaussian distribution diverges from samples of the same distribution. The uniform curve

shows how much a Gaussian approximation of a Uniform distribution drawn in the interval $(\mu_i - \sigma_i, \mu_i + \sigma_i)$ (for each i in the dimension of the underlying distribution) diverges; this serves to illustrate the divergence one would expect if attempting to model a distribution which is decidedly not normal. One would expect the baseline curve to tend to zero as the number of particles tends to infinity. Sampling error causes divergence from zero for the baseline curve. Thus we can use the baseline and uniform curves as a crude measure of normality.

In Figure 48 we see that the approximation is relatively close to the baseline. Additionally it is far removed from the uniform curve. The average divergence for the baseline, approximation and uniform curve (in nats) is: 0.035, 0.066 and 34.57 respectively. This implies that even though we are using a non-linear control technique the posterior state distributions are still approximately Gaussian.

8.5 Nonlinear System

In this section we consider the problem of controlling the full non-linear system with a linear model linearised around the unsteady operating point. The control goal is the same as before; the only difference between this section and Section 8.4 is that the underlying plant is non-linear.

The linear control model and noise parameters are the same as (113). The control tuning parameters are the same as (114).

As before we first investigate the LQG controller. The control problem is the same as (115) but this time the underlying system is non-linear. Figure 49 shows the unconstrained reference tracking results.

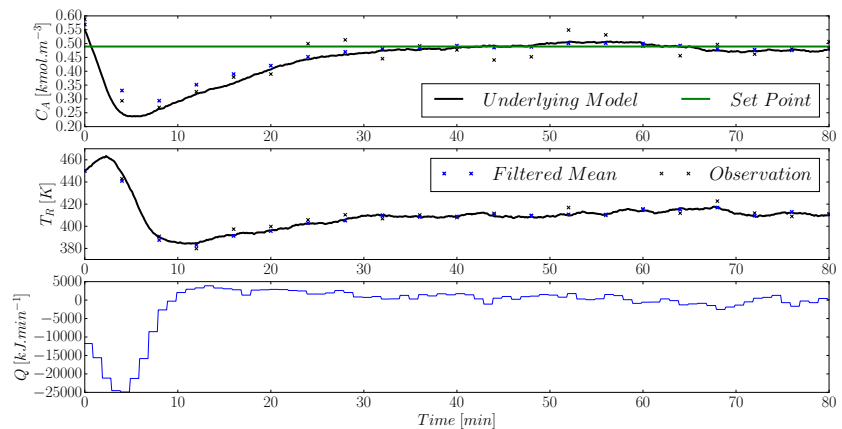


Figure 49: LQG regulator tracking with initial condition (0.55, 450) and measuring both states.

The average energy usage and concentration error was 302 kJ/min and 10.94% respectively

over the 80 min simulation time. Comparing Figures 41 and 49 we see that the maximum absolute input energy is much greater with the non-linear underlying dynamics. This is not unexpected because the controller in both cases is linear: one expects that the plant-model mismatch to have a detrimental effect on control.

In the previous section we had a linear underlying model and linear control. Figure 48 also demonstrated that the posterior state distributions were approximately Gaussian. Thus there was no reason to use non-linear inference algorithms like the Particle Filter introduced in Section 7. However, in this section we are using a non-linear underlying model and it might be advantageous to use a more sophisticated inference tool. We investigate using both a Kalman Filter and a Particle Filter for inference. In the setting of the Particle Filter we approximate the samples as Gaussian and use that for control.

As before we first investigate the deterministic MPC. The control problem is shown in (118). Note that the constraints are different due to the expected extra difficulty introduced by the non-linear underlying model.

$$\begin{aligned} \min_{\mathbf{u}} \frac{1}{2} \sum_{k=0}^{N-1} (\mu_k^T Q \mu_k + u_k^T R u_k) + \frac{1}{2} \mu_N^T P_f \mu_N \\ \text{subject to } \mu_{t+1} = A \mu_t + B u_t \\ \text{and } \begin{pmatrix} 10 \\ 1 \end{pmatrix}^T \mu_t + 400 \geq 0 \quad \forall t = 1, \dots, N \\ \text{and } |u_t| \leq 20000 \quad \forall t = 0, \dots, N-1 \end{aligned} \tag{118}$$

In Figure 50 we see that the deterministic MPC using the Kalman Filter for state inference does converge to the set point. The ability to naturally constrain the system is again highlighted in the input: as opposed to the -25 000 kJ/min required by the LQG controller the MPC manages to control the system while never requiring more than $|20000|$ kJ/min.

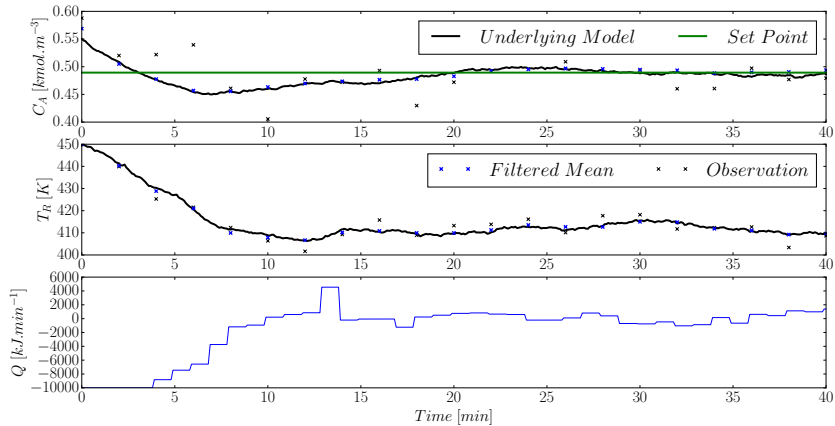


Figure 50: Deterministic constrained MPC reference tracking with initial condition $(0.55, 450)$ and measuring both states. The Kalman Filter is used for inference.

In Figure 51 we see that the state constraint is violated just like Figure 43. We also see a

somewhat unrealistic jagged state trajectory but this is just a numerical artefact. The average energy input and concentration error over the simulation run is 413 kJ/min and 14.53% respectively. Once again the added constraints explain why the performance is degraded when compared to the LQG controller.

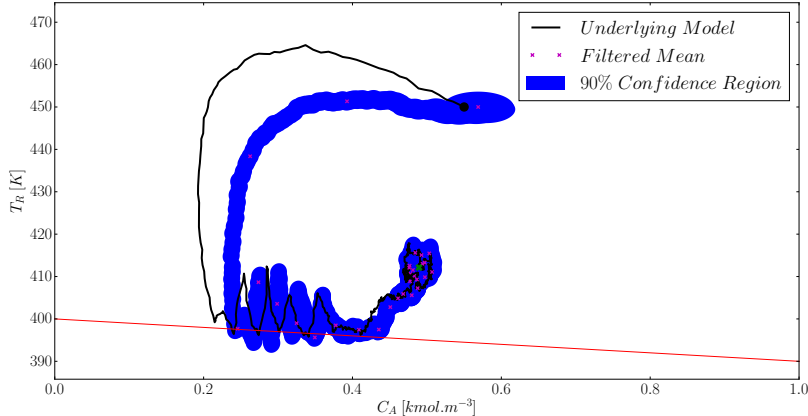


Figure 51: Deterministic constrained MPC state space trajectory with initial condition (0.55, 450) and measuring both states. The Kalman Filter is used for inference.

Since we are not using a stochastic MPC the state constraint violation is not surprising in Figure 51. However, a more significant issue is the inability of the Kalman Filter to accurately track the states throughout the simulation (the underlying system briefly diverges from the state estimates). This can be significantly problematic if a constraint existed in the left hand side of the state space: the controller wouldn't know that it was violating the constraint because the state estimate is poor. This behaviour is caused by the linear model used by the Kalman Filter. The state trajectory moves away from the region close to the linearisation point and thus, as explained in Section 6, the state estimate becomes poor.

We can remedy this situation by using a more sophisticated inference algorithm. In Figure 52 we see the deterministic MPC using a Particle Filter with 200 particles for inference.

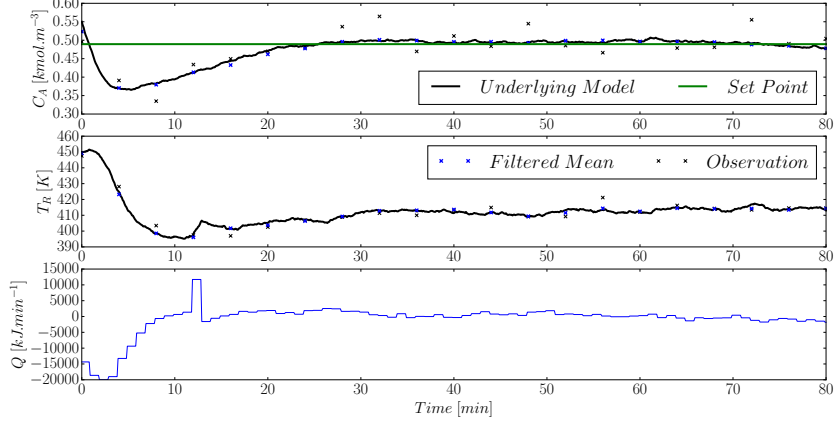


Figure 52: Deterministic constrained MPC reference tracking with initial condition $(0.55, 450)$ and measuring both states. A Particle Filter with 200 particles is used for inference.

The average energy input and concentration error is 218 kJ/min and 4.80% respectively. This is a vast improvement over the same controller where the Kalman Filter was used for inference. The benefit of accurate state estimation is apparent here and also in Figure 53.

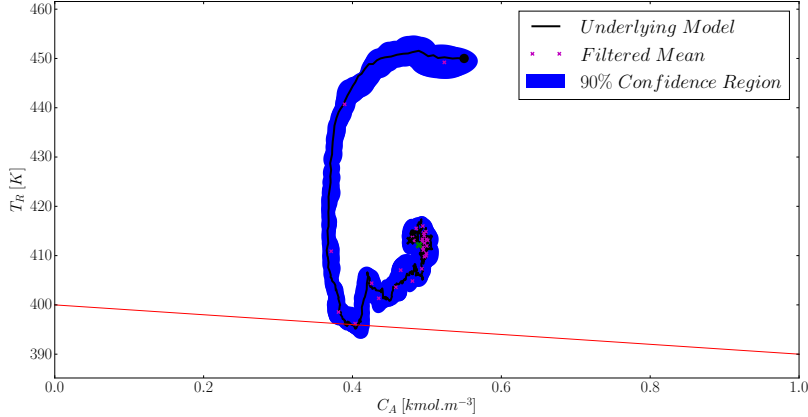


Figure 53: Deterministic constrained MPC state space trajectory with initial condition $(0.55, 450)$ and measuring both states. A Particle Filter with 200 particles is used for inference.

In Figure 51 we saw significant estimation deviation from the true underlying state, while in Figure 53 the deviation is negligible. We still have that the state constraint is violated but this is due to the stochastic nature of the underlying system. It is clear that the Particle Filter MPC combination is superior to the Kalman Filter MPC combination in this case. However, the benefit of using the Particle Filter should be weighed against the cost of the algorithm especially in higher dimensions where it is known that the Particle Filter does not perform well (recall the discussion following Figure 39).

Now we introduce the stochastically constrained MPC in (119). Note that the constraints

are different than (117) for the same reason as (118). We have $d^T = (10, 1)$ and $e = 400$ as before. By consulting a Chi-Squared Distribution table we set $k^2 = 4.6052$ which corresponds to the chance constraint $\Pr(d^T x_t + e \geq 0) \geq 90\% \forall t = 1, \dots, N$ exactly as in the previous section.

$$\begin{aligned} \min_{\mathbf{u}} \quad & \frac{1}{2} \sum_{k=0}^{N-1} (\mu_k^T Q \mu_k + u_k^T R u_k) + \frac{1}{2} \mu_N^T P_f \mu_N + \frac{1}{2} \sum_{k=0}^N \text{tr}(Q \Sigma_k) \\ \text{subject to } \quad & \mu_{t+1} = A \mu_t + B u_t \\ \text{and } \Sigma_{t+1} = & W + A \Sigma_t A^T \\ \text{and } d^T \mu_t + e \geq & k \sqrt{d^T \Sigma_t d} \forall t = 1, \dots, N \\ \text{and } |u_t| \leq & 20000 \forall t = 0, \dots, N-1 \end{aligned} \tag{119}$$

As with the deterministic case we first investigate the system where a Kalman Filter is used for inference. Figure 54 illustrates that the stochastically constrained system does indeed converge to the set point. The average energy input and concentration error is 384 kJ/min and 12.33%. The average energy usage and average concentration error is reduced compared to the deterministic system.

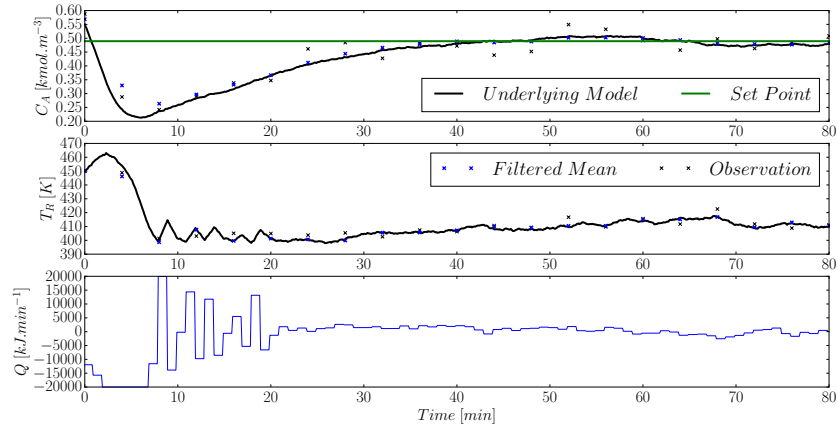


Figure 54: Stochastic constrained MPC tracking with initial condition $(0.55, 450)$ and measuring both states. A Kalman Filter is used for inference and the chance constraint is set at 90%.

Again the benefit of adding the stochastic constraint is apparent in Figure 55. It is clear that the constraint on the underlying state is not violated although the confidence region is. The margin of safety is rather small.

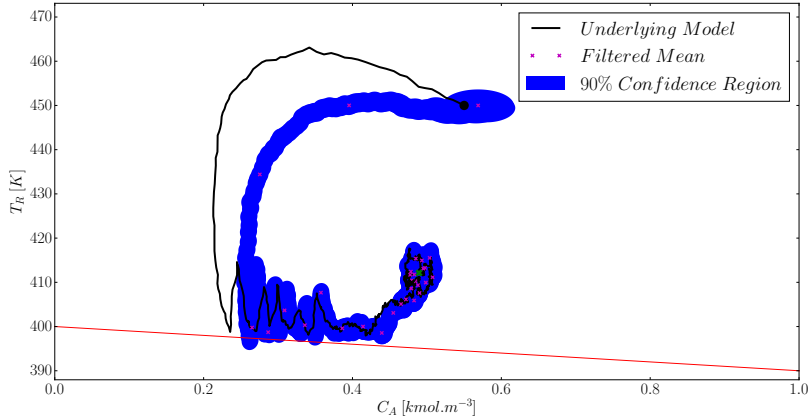


Figure 55: Stochastic constrained MPC state space trajectory with initial condition $(0.55, 450)$ and measuring both states. A Kalman Filter is used for inference and the chance constraint is set at 90%.

It is clear that the non-linearity of the underlying system makes stochastic control difficult. By increasing $k^2 = 13.8155$ which corresponds to changing the chance constraint such that $\Pr(d^T x_t + e \geq 0) \geq 99.9\% \forall t = 1, \dots, N$ we hope to increase the minimum distance between the constraint and the underlying state.

Figure 56 shows the tracking of the modified system. The average energy input and average concentration error is 358 kJ/min and 11.31% respectively. It is quite interesting that the more conservative system performs better with regard to these two metrics than the less conservative system.

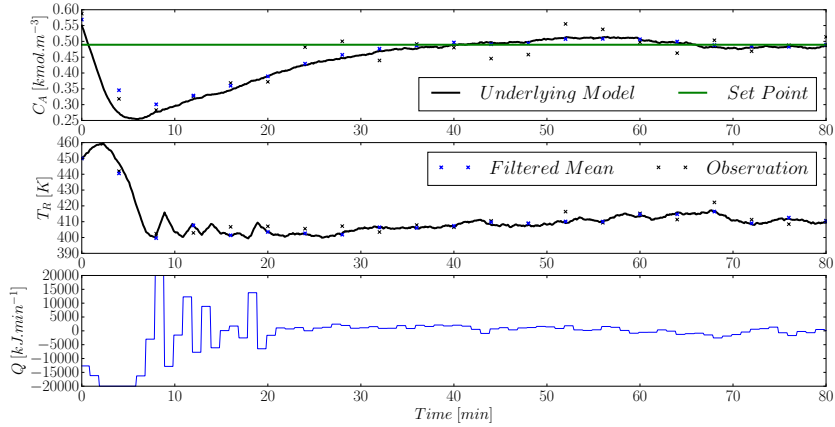


Figure 56: Stochastic constrained MPC tracking with initial condition $(0.55, 450)$ and measuring both states. A Kalman Filter is used for inference and the chance constraint is set at 99.9%.

In Figure 47 we see that the margin of safety is increased although the confidence region still spills over the constraint.

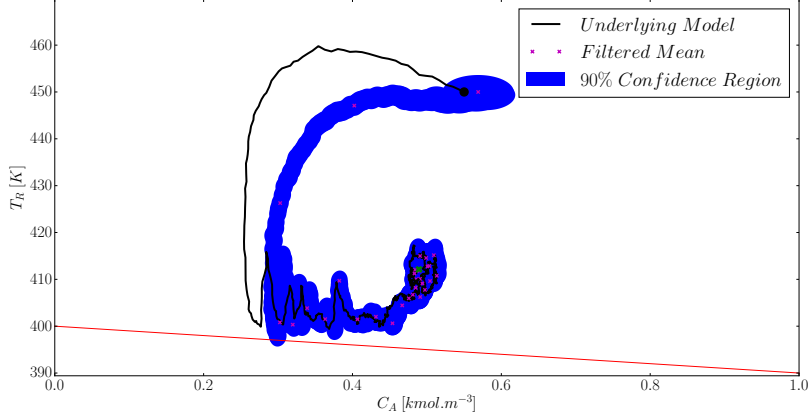


Figure 57: Stochastic constrained MPC state space trajectory with initial condition $(0.55, 450)$ and measuring both states. A Kalman Filter is used for inference and the chance constraint is set at 99.9%.

The ability of k to increase or decrease the conservativeness of the constraint lends credibility to its value, at the very least if the system is non-normal, as an empirical measure to include stochastic robustness to the MPC in an efficient way.

Figures 54 to 57 all display the undesirable property originally seen in Figure 50: the poor state estimation and associated control problems. We attempt to rectify this situation by using a more sophisticated filter with the stochastic MPC. We use the MPC as shown in (119) with a Particle filter using 200 particles. The tracking results are shown in Figure 52.

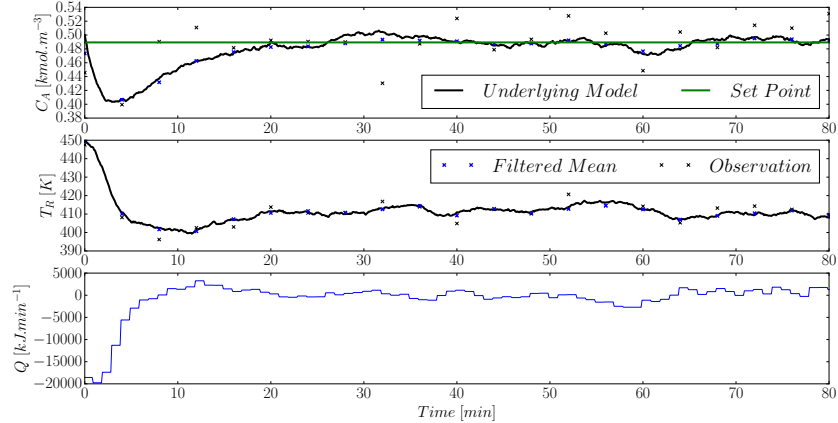


Figure 58: Stochastic constrained MPC tracking with initial condition $(0.55, 450)$ and measuring both states. A Particle Filter with 200 particles is used for inference and the chance constraint is set at 90%.

One could see the discussion in Section 7.5 as a justification for using the Particle Filter instead of the Kalman Filter for state estimation. Since the underlying model is non-linear we expect the Particle Filter to outperform the Kalman Filter (recall the discussion following

Figure 39).

The average input energy and average concentration error is 178 kJ/min and 2.98% over the course of the simulation. This is a vast improvement over the Kalman Filter MPC combination. Clearly the more accurate state estimation is immensely beneficial for control.

Figure 59 also illustrates that the stochastic constraint is easily satisfied using the more accurate estimator.

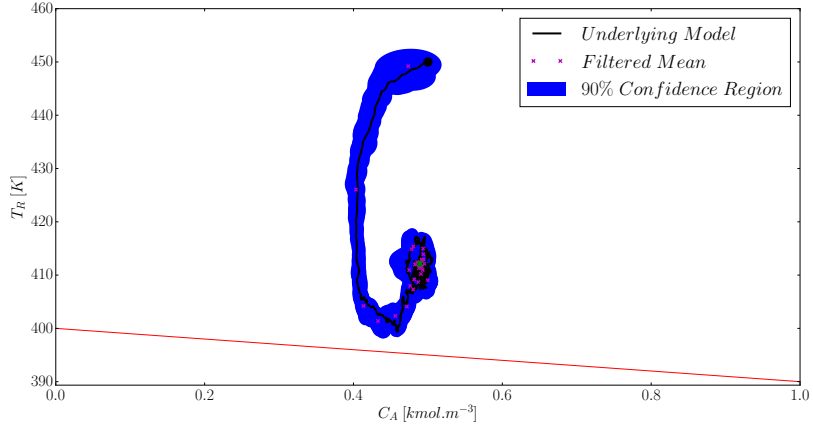


Figure 59: Stochastic constrained MPC state space trajectory with initial condition $(0.55, 450)$ and measuring both states. A Particle Filter with 200 particles is used for inference and the chance constraint is set at 90%.

As before we need to investigate the normal assumption underpinning the theory behind the chance constraint simplification. We investigate it in exactly the same manner as Figure 48 using Kullback-Leibler Divergence. To this end, Figure 60 shows the degree to which the underlying posterior state distributions are Gaussian given the non-linear underlying system.

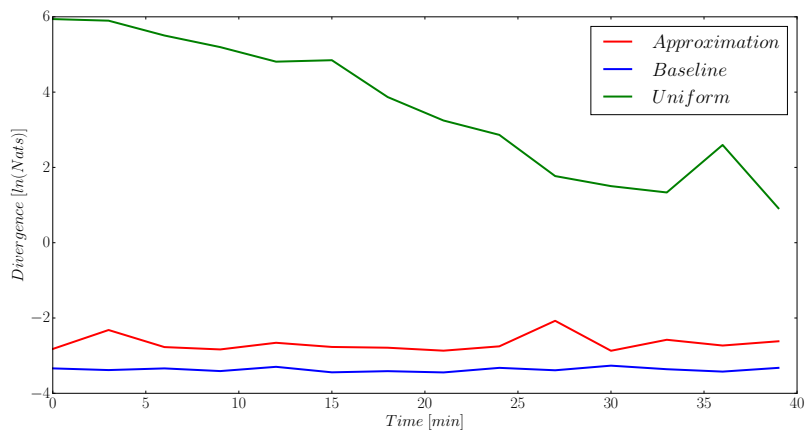


Figure 60: Kullback-Leibler Divergence between the assumed Gaussian distribution and actual distribution using 5000 particles. The underlying model is non-linear.

It is a relief that the normal assumption seems to hold almost as well in the non-linear underlying system case. The average divergence for the baseline, approximation and uniform curves are: 0.035, 0.071 and 110.11. It is not surprising that the non-linearity reduced the degree of normality of the distributions although it did not do so significantly. Therefore we can conclude that the normal assumption holds approximately.

8.6 Conclusion

We have illustrated the benefits gained by designing MPC within the framework of Probabilistic Graphical Models by showing:

1. Under the assumption of normality and linearity it is possible to convert stochastic objective functions into their deterministic equivalents. The analysis is closely related to the work of [47] and [48] but we have shown that these results are immediately obvious from within the framework of Probabilistic Graphical Models. Thus it is possible to solve LQG objective type problems without resorting to stochastic Dynamic Programming.
2. We have generalised our analysis to stochastic MPC and shown that by using the statistically important metric, the Mahalanobis Distance, we arrive at a technique for enforcing chance constraints which is very closely related to the approach taken by [44] and [45]. Under the assumptions of linearity and normality we have shown that constraint satisfaction is ensured. Due to the use of the Mahalanobis Distance metric we have provided some theoretical support for the use of the “ellipsoidal approximation” technique if the underlying system is non-linear or not exactly Gaussian.
3. Combining the previous results we have shown that it is possible to write the joint chance constrained stochastic MPC problem as a deterministic MPC problem. Additionally we show that the joint chance constraints can be written in a linear format. The entire optimisation problem can then be written in the standard form for Quadratic Programming optimisation. Standard deterministic MPC solution techniques can then be used to solve the stochastic problem.
4. We have compared the effect different inference techniques have on the quality of the MPC. If the system is linear and Gaussian the Kalman Filter is adequate. If there is significant departure from linearity or normality it can be beneficial to use the Particle Filter.

References

- [1] Y. Bar-Shalom, X.R. Li, and T. Kirubarajan. *Estimation with applications to tracking and navigation*. John Wiley and Sons, 2001.
- [2] D. Barber. Expectation correction for smoothed inference in switching linear dynamical systems. *Journal of Machine Learning*, 7:2515–2540, 2006.
- [3] D. Barber. *Bayesian Reasoning and Machine Learning*. Cambridge University Press, 2012.
- [4] I. Batina, A.A. Stoervogel, and S. Weiland. Optimal control of linear, stochastic systems with state and input constraints. In *Proceedings of the 41st IEEE Conference on Decision and Control*, 2002.
- [5] C.M. Bishop. *Pattern Recognition and Machine Learning*. Springer, 2006.
- [6] L. Blackmore, Hui Li, and B. Williams. A probabilistic approach to optimal robust path planning with obstacles. In *American Control Conference*, June 2006.
- [7] L. Blackmore, O. Masahiro, A. Bektassov, and B.C. Williams. A probabilistic particle-control approximation of chance-constrained stochastic predictive control. *IEEE Transactions on Robotics*, 26, 2010.
- [8] M. Cannon, B. Kouvaritakis, and X. Wu. Probabilistic constrained mpc for multiplicative and additive stochastic uncertainty. *IEEE Transactions on Automatic Control*, 54(7), 2009.
- [9] A.L. Cervantes, O.E. Agamennoni, and J.L Figueroa. A nonlinear model predictive control system based on weiner piecewise linear models. *Journal of Process Control*, 13:655–666, 2003.
- [10] R. Chen and J.S. Liu. Mixture kalman filters. *Journal of Royal Statistical Society, Series B*, 62(3):493–508, 2000.
- [11] B.N. Datta. *Numerical Methods for Linear Control Systems - Design and Analysis*. Elsevier, 2004.
- [12] M. Davidian. Applied longitudinal data analysis. North Carolina State University, 2005.
- [13] R. De Maesschalck, D. Jouan-Rimbaus, and D.L. Massart. Tutorial: The mahalanobis distance. *Chemometrics and Intelligent Laboratory Systems*, 50:1–18, 2000.
- [14] N. Deo. *Graph Theory with Applications to Engineering and Computer Science*. Prentice-Hall, 1974.
- [15] A. Doucet and A.M. Johansen. A tutorial on particle filtering and smoothing: fifteen years later. Technical report, The Institute of Statistical Mathematics, 2008.

- [16] A.D. Doucet, N.J. Gordon, and V. Krishnamurthy. Particle filters for state estimation of jump markov linear systems. *IEEE Transactions on Signal Processing*, 49(3):613–624, March 2001.
- [17] J. Du, C. Song, and P. Li. Modeling and control of a continuous stirred tank reactor based on a mixed logical dynamical model. *Chinese Journal of Chemical Engineering*, 15(4):533–538, 2007.
- [18] The Economist. In praise of bayes. Article in Magazine, September 2000.
- [19] H.C. Edwards and D.E. Penny. *Elementary Differential Equations*. Pearson, 6th edition edition, 2009.
- [20] W. Forst and D. Hoffmann. *Optimisation - Theory and Practice*. Springer, 2010.
- [21] O.R. Gonzalez and A.G. Kelkar. *Electrical Engineering Handbook*. Academic Press, 2005.
- [22] N.J. Gordon, D.J. Salmond, and A.F.M. Smith. Novel approach to nonlinear/non-gaussian bayesian state estimation. *IEE Proceedings-F*, 140(2):107–113, 1993.
- [23] K. Ito and K. Xiong. Gaussian filters for nonlinear filtering problems. *IEEE Transactions on Automatic Control*, 45(5):910–928, 2000.
- [24] R. J. Jang and C.T. Sun. *Neuro-fuzzy and soft computing: a computational approach to learning and machine intelligence*. Prentice-Hall, 1996.
- [25] D. Koller and N. Friedman. *Probabilistic Graphical Models*. MIT Press, 2009.
- [26] K. B. Korb and A. E. Nicholson. *Bayesian Artificial Intelligence*. Series in Computer Science and Data Analysis. Chapman & Hall, first edition edition, 2004.
- [27] M. Kvasnica, M. Herceg, L. Cirka, and M. Fikar. Model predictive control of a cstr: a hybrid modeling approach. *Chemical Papers*, 64(3):301–309, 2010.
- [28] U.N. Lerner. *Hybrid Bayesian Networks for Reasoning about Complex Systems*. PhD thesis, Stanford Univesity, 2002.
- [29] P. Li, M. Wendt, H. Arellano-Garcia, and G. Wozny. Optimal operation of distillation processes under uncertain inflows accumulated in a feed tank. *American Institute of Chemical Engineers*, 2002.
- [30] P. Li, M. Wendt, and G. Wozny. A probabilistically constrained model predictive controller. *Automatica*, 38:1171–1176, 2002.
- [31] W.L. Luyben. *Process Modeling, Simulation and Control for Chemical Engineers*. McGraw-Hill, 2nd edition edition, 1990.
- [32] J.M. Maciejowski. *Predictive Control with constraints*. Prentice-Hall, 2002.

- [33] O. Masahiro. Joint chance-constrained model predictive control with probabilistic resolvability. *American Control Conference*, 2012.
- [34] P. Mhaskar, N.H. El-Farra, and P.D. Christofides. Stabilization of nonlinear systems with state and control constraints using lyapunov-based predictive control. *Systems and Control Letters*, 55:650–659, 2006.
- [35] K.P. Murphy. Switching kalman filters. Technical report, Compaq Cambridge Research Lab, 1998.
- [36] K.P. Murphy. *Dynamic Bayesian Networks: Representation, Inference and Learning*. PhD thesis, University of California, Berkeley, 2002.
- [37] K.P. Murphy. *Machine Learning: A Probabilistic Perspective*. MIT Press, 2012.
- [38] T. Pan, S. Li, and W.J. Cai. Lazy learning based online identification and adaptive pid control: a case study for cstr process. *Industrial Engineering Chemical Research*, 46:472–480, 2007.
- [39] J.B. Rawlings and D.Q. Mayne. *Model Predictive Control*. Nob Hill Publishing, 2009.
- [40] B. Reiser. Confidence intervals for the mahalanobis distance. *Communications in Statistics: Simulation and Computation*, 30(1):37–45, 2001.
- [41] A.T. Schwarm and Nikolaou. Chance constrained model predictive control. Technical report, University of Houston and Texas A&M University, 1999.
- [42] C. Snyder, T. Bengtsson, P. Bickel, and J. Anderson. Obstacles to high-dimensional particle filtering. *Mathematical Advances in Data Assimilation*, 2008.
- [43] S.J. Streicher, S.E. Wilken, and C. Sandrock. Eigenvector analysis for the ranking of control loop importance. *Computer Aided Chemical Engineering*, 33:835–840, 2014.
- [44] D.H. van Hessem and O.H. Bosgra. Closed-loop stochastic dynamic process optimisation under input and state constraints. In *Proceedings of the American Control Conference*, 2002.
- [45] D.H. van Hessem, C.W. Scherer, and O.H. Bosgra. Lmi-based closed-loop economic optimisation of stochastic process operation under state and input constraints. In *Proceedings of the 40th IEEE Conference on Decision and Control*, 2001.
- [46] R.S. Wills. Google’s pagerank: the math behind the search engine. Technical report, North Carolina State University, 2006.
- [47] J. Yan and R.R. Bitmead. Model predictive control and state estimation: a network example. In *15th Triennial World Conference of IFAC*, 2002.
- [48] J. Yan and R.R. Bitmead. Incorporating state estimation into model predictive control and its application to network traffic control. *Automatica*, 41:595–604, 2005.

- [49] M.B. Yazdi and M.R. Jahed-Motlagh. Stabilization of a cstr with two arbitrarily switching modes using model state feedback linearisation. *Chemical Engineering Journal*, 155(3):838–843, 2009.